PROCEEDINGS OF SCIENCE

CP violation studies at Belle (including UT angles)

Kentaro Negishi[*†]
Tohoku Univercity
E-mail: negishi@epx.phys.tohoku.

The Belle experiment was opareting the data taking from May 1999 to 2010. Belle performed a large number of measurements related to *CP* violation. Some of achievements of those measurements are reviewed, especially measurements for the angles of the unitarity triangle.

The XIth International Conference on Heavy Quarks and Leptons,
June 11-15, 2012
Prague, Czech Republic

*Speaker.
†A footnote may follow.

PoS(HQL 2012)040

1. Introduction

Determination of the parameters in the standard model is important as a consistency check and as a way to search for new physics. In the standard model, Cabibbo-Kobayashi-Maskawa (CKM) matrix [1] gives a successful description of current experimental measurements of *CP* violation. The CKM matrix is written as [2]

$$\begin{pmatrix} V_{ud} & V_{us} & V_{ub} \\ V_{cd} & V_{cs} & V_{cb} \\ V_{td} & V_{ts} & V_{tb} \end{pmatrix} = \begin{pmatrix} 1-\lambda^2/2 & \lambda & A\lambda^3(\rho - i\eta) \\ -\lambda & 1-\lambda^2/2 & A\lambda^2 \\ A\lambda^3(1-\rho-i\eta) & -A\lambda^2 & 1 \end{pmatrix}, \tag{1.1}$$

where V_{ub} and V_{td} have *CP* violating complex phases. Due to the unitarity condition of this matrix, the following relation is expected to hold:

$$V_{td}V_{tb}^* + V_{cd}V_{cb}^* + V_{ud}V_{ub}^* = 0. \tag{1.2}$$

CP violation in *B* meson decays are related to the angles ϕ_1, ϕ_2 and ϕ_3 defined as shown in Fig. 1. Here, the phase of V_{td} plays a fundamental role to cause *CP* violation by the interference with V_{cb} and V_{ub} resulting in determination of the *CP* violating angles ϕ_1 and ϕ_2, respectively. The angle ϕ_3 can be determined by the direct *CP* asymmetries in $B \to DK$ decays. Since *b* quark belongs to the third generation of quarks, many decay modes of *B* meson are available, but the branching fraction to the modes usable for *CP* violation is limited. Thus, a large number of *B* mesons have to be produced to investigate *CP* violation in the *b*-quark system.

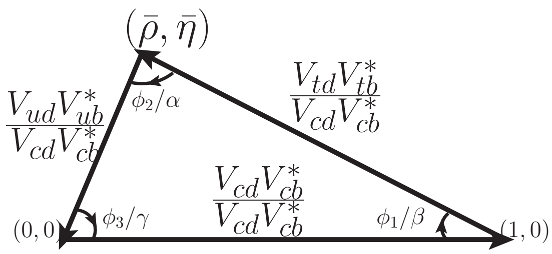

Figure 1: The unitarity triangle. The *CP* violation parameters are defined as the angles ϕ_1, ϕ_2 and ϕ_3.

In order to investigate the *CP* violation mechanism, the asymmetric-energy e^+e^- collider *B*-factory machine, KEKB was build at KEK in 1999. KEKB recorded a peak luminosity of 2.11×10^{34} cm^{-2}s^{-1}, and a integrated luminosity reached 1041 fb^{-1} in the total. The recorded number of *B* meson pairs has been found to be 772×10^6 $B\bar{B}$ pairs at the $\Upsilon(4S)$ resonance with the Belle detector. In this report, we discuss experimental tests of the CKM theory and search for new physics through time-dependent and independent measurements in the *B* meson system, especially the measurements of *CP* violating angles ϕ_1, ϕ_2 and ϕ_3 using the full $\Upsilon(4S)$ data sample collected.

2. Time-dependent measurements in *B* meson system

By a measurement of time evolution of *B* meson pairs, we can give constraints on the *CP* violating angles, ϕ_1 and ϕ_2. In the decay chain $\Upsilon(4S) \to B^0\bar{B}^0 \to f_{\rm CP} f_{\rm tag}$, where one of the *B* meson decays at time $t_{\rm CP}$ to a CP eigenstate $f_{\rm CP}$ and the other decay at time $t_{\rm tag}$ to final state $f_{\rm tag}$ that distinguishes between B^0 and $\bar{B}^0$, the decay rate has a time dependence on the $\Upsilon(4S)$ rest frame given by

$$\mathscr{P}(\Delta t) = \frac{e^{-\frac{|\Delta t|}{\tau_{B^0}}}}{4\tau_{B^0}}\{1 + q\cdot[\mathscr{S}\sin(\Delta m_d \Delta t) + \mathscr{A}\cos(\Delta m_d \Delta t)]\}. \tag{2.1}$$

Here $\mathscr{S}$ and $\mathscr{A}$ are CP violation parameters, τ_{B^0} is the B^0 lifetime, Δm_d is the mass difference between the two neutral B mass eigenstates, $\Delta t = t_{\rm CP} - t_{\rm tag}$, and the b-flavor charge $q = +1(-1)$ when the tagging B meson is a $B^0(\bar{B}^0)$. By selecting the neutral B decays into $f_{\rm CP}$ via the amplitudes containing no complex phase, CP violation is caused by the interference between decay and V_{td} in mixing, where the angle ϕ_1 arises as a result of the interference.

Instead of the B decays into $f_{\rm CP}$, collecting the events in which one neutral B meson decays into the flavor-specific final state enables us to determine the B^0-$\bar{B}^0$ mixing parameter Δm_d, by measuring opposite and same flavor asymmetry as function of Δt. The mixing-induced CP violation parameter $\mathscr{S}$ gives essential information for the angles ϕ_1 and ϕ_2. The experimental determinations will be reviewed from the next section in detail.

3. Measurement of $\sin 2\phi_1$

For the $b \to c\bar{c}s$ transition induced decay of the neutral B meson such as $B^0 \to (c\bar{c})K^0$, the standard model predicts $\mathscr{S} = -\xi_f \sin 2\phi_1$ and $\mathscr{A} = 0$ with very small theoretical uncertainty [3], where $\xi_f = +1(-1)$ corresponds to CP-even(-odd) final states, and ϕ_1 is defined as $\phi_1 \equiv \arg(-V_{cd}V_{cb}^*/V_{td}V_{tb}^*)$.

Belle has updated $\sin 2\phi_1$ measurement with the full dataset (772×10^6 $B\bar{B}$ pairs) [4]. The B decays into the CP-odd eigenstates, $f_{\rm CP} = J/\psi K_S$, $\psi(2S)K_S$ and $\chi_{c1}K_S$, and the CP-even eigenstate, $f_{\rm CP} = J\psi K_L$ are reconstructed. As shown in Fig. 2, the $B^0 \to f_{\rm CP}$ decay signal other than $J\psi K_L$ is identified by two kinematic variables calculated in the $\Upsilon(4S)$ resonance rest frame (CMS): the energy difference $\Delta E \equiv E_B^* - E_{\rm beam}^*$ and the beam-energy constrained mass $M_{\rm bc} \equiv \sqrt{(E_{\rm beam}^*)^2 - (p_B^*)^2}$, where $E_{\rm beam}^*$ is the beam energy in the CMS, and E_B^* and p_B^* are the CMS energy and momentum of the reconstructed B candidate, respectively. $B^0 \to J/\psi K_L$ candidates are identified by the value of p_B^* calculated using a two-body decay kinematic assumption. The b-quark flavor is identified using a flavor tagging routine described in Ref. [5]. An unbinned maximum likelihood fit is performed to the Δt distribution using Eq.(2.1), where the Δt distribution is convolved with the proper-time interval resolution function [6]. The two CP violation parameters, $\sin 2\phi_1 = -\xi_f \mathscr{S}$ and $\mathscr{A}$ are obtained to be

$$\sin 2\phi_1 = 0.667 \pm 0.023({\rm stat}) \pm 0.012({\rm syst}), \tag{3.1}$$

$$\mathscr{A} = 0.006 \pm 0.016({\rm stat}) \pm 0.012({\rm syst}). \tag{3.2}$$

The background-subtracted Δt distribution for $q = +1(-1)$ events and asymmetry are shown in Fig. 3.

4. Determination of ϕ_2

In B decays into proper $f_{\rm CP}$ mediated by the $b \to u$ transition, its complex phase interferes with B^0-$\bar{B}^0$ mixing and results in the CP violation which can be determined to be the angle ϕ_2. A lot of

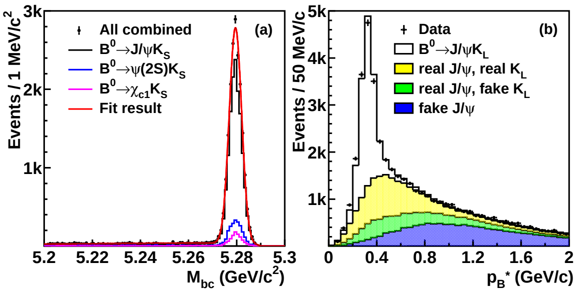

Figure 2: (color online) $M_{\rm bc}$ distribution within the ΔE signal region for $B^0 \to J/\psi K_S$ (black), $\psi(2S)K_S$ (blue) and $\chi_{c1}K_S$ (magenta), the superimposed curve (red) shows the fit result from all those modes combined (left) and p_B^* distribution of $B^0 \to J/\psi K_L$ candidates with the results of the fit separately indicated as signal (open histogram), background events with a real J/ψ and a real K_L (yellow), with a real J/ψ and a fake K_L (green) and with a fake J/ψ (blue) (right).

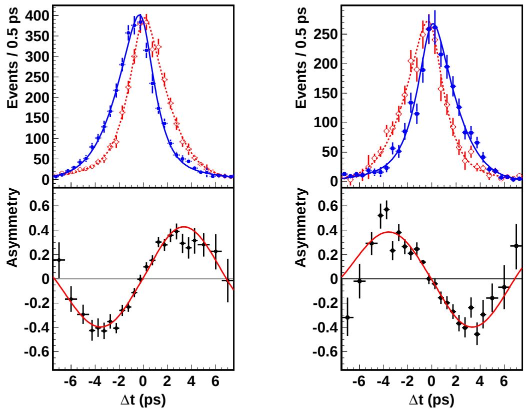

Figure 3: (color online) The background-subtracted Δt distribution for $q = +1$ (red) and $q = -1$ (blue) events and asymmetry for good tag quality events in $(c\bar{c})K_S$ (left) and $J/\psi K_L$ (right) cases.

measurements have been performed so far to constrain ϕ_2, where some important decay modes are used, such as B decays to $\pi\pi$, $\rho\rho$ and $\rho\pi$. In such decay processes, direct CP violation is possible, $\mathscr{A} \neq 0$, due to a large contribution from the electroweak penguin-mediated decay processes. Due to this penguin contribution, the time-dependent measurement can only give the information on the effective angle $\phi_2^{\rm eff}$, rather than ϕ_2 itself. However, the shift, $\Delta\phi_2 = \phi_2 - \phi_2^{\rm eff}$ can be determined by an SU(2) isospin analysis [7] or SU(3) flavor symmetry [8]. Using the $\pi\pi$, $\rho\rho$ and $\rho\pi$ modes, ϕ_2 is determined to be $\phi_2 = (89.0^{+4.4}_{-4.2})^\circ$ [9].

4.1 Other possibility to determine ϕ_2

The branching fraction and CP violation parameters are measured in $B^0 \to a_1(1260)^\pm\pi^\mp$ decays [10]. The decay $B^0 \to a_1^\pm\pi^\mp$ is reconstructed using $a_1^\pm$ that is reconstructed from $\pi^\pm\pi^+\pi^-$, and additional $\pi^\mp$. We obtain the branching fraction of $\mathscr{B}(B^0 \to a_1^\pm(1260)\pi^\mp) \times \mathscr{B}(a_1^\pm(1260) \to \pi^\pm\pi^+\pi^-)$ to be $(11.1 \pm 1.0 \pm 1.4) \times 10^{-6}$ from a 4-dimensional fit to the kinematic variables: ΔE, a Fisher discriminant variable for $e^+e^- \to q\bar{q}$ $(q = u,d,s,c)$ background suppression, $m_{3\pi}$ and

$\mathcal{H}_{3\pi}$ as shown in Fig. 4, where $\mathcal{H}_{3\pi}$ is cosine of the helicity angle of the 3 π. Figure 5 shows the

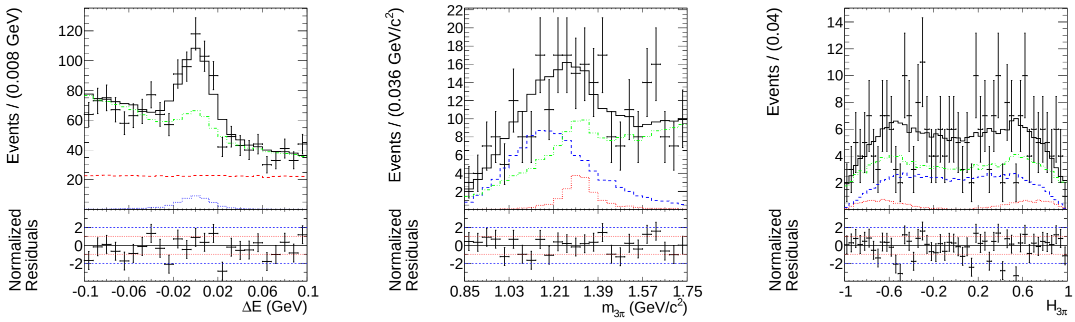

Figure 4: (color online) Projections of the fit to the $B^0 \to a_1^{\pm}\pi^{\mp}$ data for the data (points with error bars) and fit result (solid black). The left figure shows the ΔE projection for the peaking background (dotted blue), the $q\bar{q}$ background (dashed red) and the total background (dashed-dotted green). The middle and right figures show the $m_{3\pi}$ and $\mathcal{H}_{3\pi}$ projections, for the $a_1^{\pm}$ contribution (dashed blue), the the $a_2^{\pm}$ contribution (dotted red) and the total background (dashed-dotted green), respectively.

background-subtracted time-dependent fit results for $B^0 \to a_1^{\pm}\pi^{\mp}$.

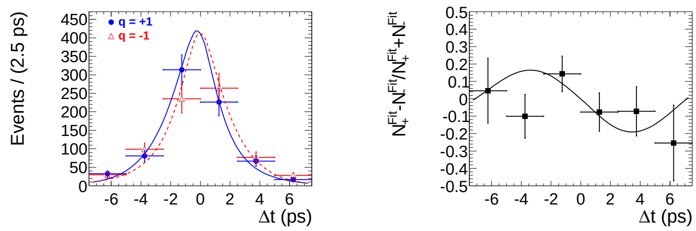

Figure 5: The results of the Δt distribution and asymmetry in $a_1^{\pm}\pi^{\mp}$.

In a time-dependent measurement to extract *CP* asymmetry, we obtain the *CP* violation parameters

$$\mathcal{S} = -0.51 \pm 0.14 \pm 0.08, \tag{4.1}$$

$$\mathcal{A} = -0.06 \pm 0.05 \pm 0.07, \tag{4.2}$$

where we find first evidence of mixing-induced *CP* violation in $B^0 \to a_1(1260)^{\pm}\pi^{\mp}$ decays with 3.1σ significance. However, there is no evidence for time and flavor integrated direct *CP* violation.

5. ϕ_3 measurements from $B \to DK$

In the usual quark-phase convention where large complex phases appear only in V_{ub} and V_{td}, the measurement of ϕ_3 is equivalent to the extraction of the phase of V_{ub} relative to the phases of other CKM matrix elements. To date, the ϕ_3 measurement has been advanced mainly by exploiting B meson decays into $D^{(*)}K$ channel, shown in Fig. 6, wherein the *CP* sensitivity is due to the

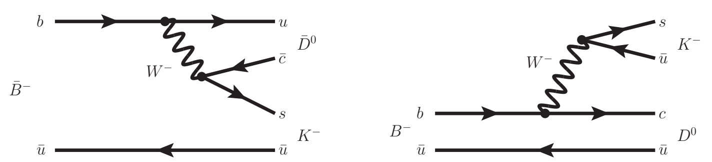

Figure 6: Diagrams for the $B^- \to D^{(*)0}K^-$ and $B^- \to \bar{D}^{(*)0}K^-$ decays. The ϕ_3 dependence in the $b \to u$ transition is extracted from the interference of the two decay paths, which occurs when the $\bar{D}^0$ and D^0 mesons decay to the same final state.

interference between the two amplitudes of $\bar{D}^{(*)0}$ and $D^{(*)0}$ decays into a common final state. We define the magnitude of the ratio of amplitudes $r_B = |A(B^- \to \bar{D}^0K^-)/A(B^- \to D^0K^-)|$ and the strong phase difference $\delta_B = \delta(B^- \to \bar{D}^0K^-) - \delta(B^- \to D^0K^-)$, which are crucial parameters needed for the extraction of ϕ_3.

5.1 Results for $B^- \to D^{(*)}K^-$, $D \to K_S\pi\pi$

One of the most promising ways of measuring ϕ_3 uses the decay $B^- \to D^{(*)}K^-$, $D \to K_S\pi\pi$, where $D^{(*)}$ indicates $D^{(*)0}$ or $\bar{D}^{(*)0}$, and is called GGSZ method [11]. The method is based on the fact that the amplitudes for $B^\pm$ can be expressed by

$$M_\pm = f(m_\pm^2, m_\mp^2) + r_B e^{\pm i\phi_3 + i\delta_B} f(m_\mp^2, m_\pm^2), \tag{5.1}$$

where $m_\pm^2$ are defined as Dalitz plot variables $m_\pm^2 = m_{K_S\pi^\pm}^2$, and $f(m_+^2, m_-^2)$ is the amplitude of the $\bar{D}^0 \to K_S\pi^+\pi^-$ decay. By applying a fit on $m_\pm^2$, ϕ_3 is extracted with r_B and δ_B.

Using obtained amplitude $f(m_+^2, m_-^2)$ and background fractions, the fit on $m_\pm^2$ is performed with the parameters $x_\pm = r_B\cos(\pm\phi_3 + \delta_B)$ and $y_\pm = r_B\sin(\pm\phi_3 + \delta_B)$. The amplitude $f(m_+^2, m_-^2)$ is obtained by a large sample of $D \to K_s\pi^+\pi^-$ decays produced in continuum e^+e^- annihilation. The background fractions are determined depending on ΔE, $M_{\rm bc}$ and event-shape variables for $q\bar{q}$ backgrounds suppression. The most precise ϕ_3 measurement from Belle is based on a data sample that contains 657×10^6 $B\bar{B}$ pairs [12]. From this measurements,

$$\phi_3 = (78.4^{+10.8}_{-11.6}(\text{stat}) \pm 3.6(\text{syst}) \pm 8.9(\text{model}))^\circ, \tag{5.2}$$

as well as $r_B = 0.161^{+0.040}_{-0.038} \pm 0.011^{+0.050}_{-0.010}$, $r_B^* = 0.196^{+0.073}_{-0.072} \pm 0.013^{+0.062}_{-0.012}$, $\delta_B = (137.4^{+13.0}_{-15.7} \pm 4.0 \pm 22.9)^\circ$ and $\delta_B^* = (341.7^{+18.6}_{-20.9} \pm 3.2 \pm 22.9)^\circ$ are obtained. The third error is the model uncertainty which comes from imperfect description of the observable D^0 Dalitz plot distribuiton, and uncertainty of the phase of the complex amplitude f.

To overcome the large model uncertainty, a model-independent approach has been performed using the full dataset of 772×10^6 $B\bar{B}$ pairs [13]. The measurement uses $B^\pm \to DK^\pm$ decays with the neutral D meason decaying to $K_S\pi^+\pi^-$. Dalitz plane is divided into 16 bins as shown in the left plot of Fig. 7. For each bin, the magnitude of the D decay amplitude is determined from tagged sample of $D^0 \to h^+h^-$, and the phase is determined from coherent state of $D^0\bar{D}^0$ produced from $\psi(3770)$, both of which are done by CLEO collaboration [14]. In the middle plot of Fig. 7, we show the $B^\pm$ signal yields and the difference of them in each bin. Combining the D decay amplitudes and the $B^{\pm}$ yields in all bins, the parameters $x_{\pm}$ and $y_{\pm}$ are obtained as shown in the right plot of Fig. 7. The angle ϕ_3 is measured to be

$$\phi_3 = (77.3^{+15.1}_{-14.9}(\text{stat}) \pm 4.2(\text{syst}) \pm 4.3(D \text{ decay phase}))^{\circ}. \tag{5.3}$$

A factor responsible for lower statistical sensitivity compared to the result in Eq.(5.2), despite the increase of the data size, is as intrinsic poorer statistical precision in the binning approach. The sources of the systematic error are limited by the statistics of the control channels. The third error is due to the uncertainties of the phase of the D decay amplitude, and is expected to decrease to 1° or less by using data sample of BES Ⅲ experiment.

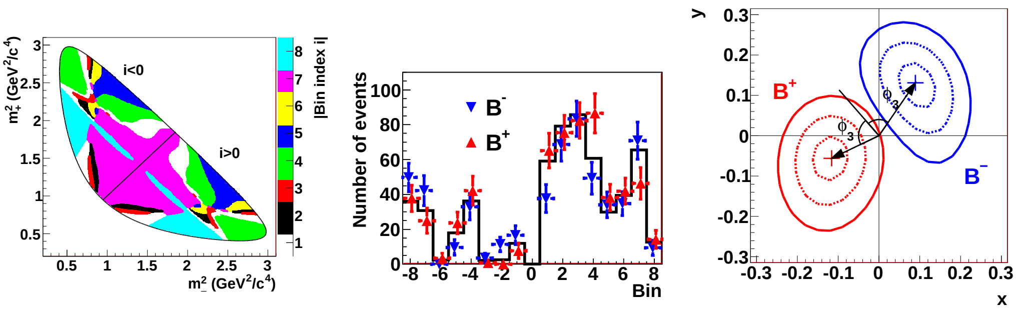

Figure 7: (color online) Binning of the Dalitz plane for $D \to K_S\pi^+\pi^-$ (left). and one index corresponds to two regions. Number of signal events for the B^- (blue) and B^+ (red) decays in each bin (middle), and number of events for flavor sample (histogram). Fit result on the parameters $x_{\pm}$ and $y_{\pm}$ (right), where the contours for one, two and three standard deviations are shown. The weak phase ϕ_3 appears as half the opening angle between (x_+, y_+) and (x_-, y_-) vectors.

5.2 Results for GLW modes

In one of proposed methods to extract ϕ_3 [15], the branching fractions $\mathscr{B}(B^- \to \bar{D}^0 K^-)$, $\mathscr{B}(B^- \to D^0 K^-)$ and $\mathscr{B}(B^- \to D_{CP+} K^-)$, where $D_{CP+} = (D^0 + \bar{D}^0)/\sqrt{2}$, are separately measured. This method makes use of the relation that the phase difference between the amplitudes $A(B^- \to \bar{D}^0 K^-)$ and $A(B^- \to D^0 K^-)$ becomes $\delta_B - \phi_3$, while the one for B^+ decays becomes $\delta_B + \phi_3$. The branching fraction $\mathscr{B}(B^- \to \bar{D}^0 K^-)$ becomes relatively smaller than the branching fraction $\mathscr{B}(B^- \to D^0 K^-)$, if ϕ_3 is non-zero. On top of that, additional constraint is obtained from the decay $B^- \to D_{CP-} K^-$, where $D_{CP-} = (D^0 - \bar{D}^0/\sqrt{2})$. Usual experimental observables are

$$\begin{aligned} \mathscr{R}_{CP\pm} &\equiv \frac{\mathscr{B}(B^- \to D_{CP\pm} K^-) + \mathscr{B}(B^+ \to D_{CP\pm} K^+)}{\mathscr{B}(B^- \to D^0 K^-) + \mathscr{B}(B^+ \to \bar{D}^0 K^+)} \\ &= 1 + r_B^2 + 2 r_B \cos\delta_B \cos\phi_3, \end{aligned} \tag{5.4}$$

$$\begin{aligned} \mathscr{A}_{CP\pm} &\equiv \frac{\mathscr{B}(B^- \to D_{CP\pm} K^-) - \mathscr{B}(B^+ \to D_{CP\pm} K^+)}{\mathscr{B}(B^- \to D_{CP\pm} K^-) + \mathscr{B}(B^+ \to D_{CP\pm} K^+)} \\ &= 2 r_B \sin\delta_B \sin\phi_3 / \mathscr{R}_{CP\pm}. \end{aligned} \tag{5.5}$$

Belle has updated the measurement of these observables based on the full dataset that contains 772×10^6 $B\bar{B}$ pairs [16]. We obtained $\mathscr{R}_{CP+} = 1.03 \pm 0.07 \pm 0.03$, $\mathscr{R}_{CP-} = 1.13 \pm 0.09 \pm 0.05$, $\mathscr{A}_{CP+} = +0.29 \pm 0.06 \pm 0.02$ and $\mathscr{A}_{CP-} = -0.12 \pm 0.06 \pm 0.01$. The fit result is shown in Fig. 8.

The result for $\mathscr{A}_{CP+}$ is the evidence of the direct CP violation. The ϕ_3 determination is possible if the GLW observables are combined with the measurements from the ADS method.

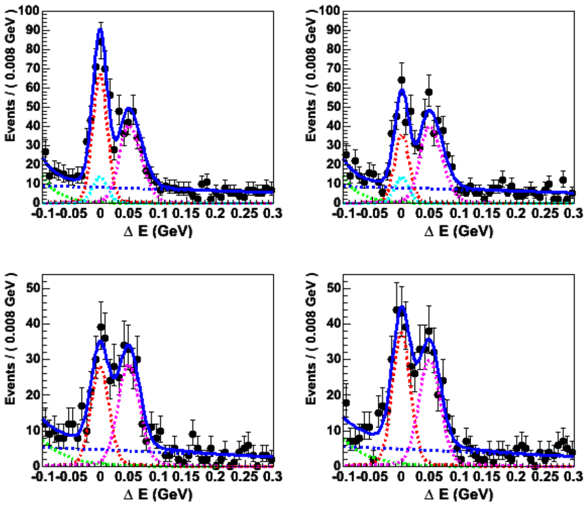

Figure 8: (color online) Fit results of ΔE distributions for $D \to KK$, $\pi\pi$ CP-even and $D \to K_S\pi^0$, $K_S\eta$ CP-odd modes. The left and right columns show B^- and B^+ results, respectively. Signal component (red) is located at around $\Delta E = 0$ GeV on non-resonant three-body component (aqua), $B^\pm \to D\pi^\pm$ component (magenta) is located at around $\Delta E = 0.05$ GeV, and $B\bar{B}$ (green) and $q\bar{q}$ (blue) background components are located in the entire region.

5.3 Results for ADS mode

The effect of CP violation can be enhanced, if the final state of the D decay following to the $B^- \to DK^-$ is chosen that the interfering amplitudes have comparable magnitudes [17]. The decay $D \to K^+\pi^-$ is a particularly useful mode; the usual observables are the partial rate $\mathscr{R}_{DK}$ and the CP-asymmetry $\mathscr{A}_{DK}$. Here, $\mathscr{R}_{DK}$ and $\mathscr{A}_{DK}$ correspond to what are changed (1, δ_B) into (r_D, $\delta_B + \delta_D$) of the low of cosines of the $\mathscr{R}_{CP}$ and $\mathscr{A}_{CP}$. $r_D = |A(D^0 \to K^+\pi^-)/A(D^0 \to K^-\pi^+)|$, and $\delta_D = \delta(D^0 \to K^-\pi^+) - \delta(D^0 \to K^+\pi^-)$. For the parameters r_D and δ_D, external experimental inputs can be used [18]. The first evidence of CP violating signal in $B^- \to DK^-$ is obtained at Belle [19].

5.3.1 Results for $\bar{B}^0 \to D\bar{K}^{*0}$, $D \to K^+\pi^-$ and $\bar{K}^{*0} \to K^-\pi^+$

One of the possible modes which can be used to extract ϕ_3 is $\bar{B}^0 \to D\bar{K}^{*0}$, followed by $D \to K^+\pi^-$ and $\bar{K}^{*0} \to K^-\pi^+$. In this analysis, b-quark flavor is tagged by the charge of K from K^* candidate, and there is possibility to observe larger CP violation than charged $B^- \to DK^{(*)-}$, since the amplitude of interference between $\bar{B}^0 \to D^0\bar{K}^{*0}$ and $\bar{B}^0 \to \bar{D}^0\bar{K}^{*0}$ is large. Usual observables are defined as

$$\mathscr{R}_{DK^*} \equiv \frac{\mathscr{B}(\bar{B}^0\to[K^+\pi^-]_D K^-\pi^+)+\mathscr{B}(B^0\to[K^-\pi^+]_D K^+\pi^-)}{\mathscr{B}(\bar{B}^0\to[K^-\pi^+]_D K^-\pi^+)+\mathscr{B}(B^0\to[K^+\pi^-]_D K^+\pi^-)} = r_S^2 + r_D^2 + 2kr_S r_D \cos(\delta_S+\delta_D)\cos\phi_3, \quad (5.6)$$

$$\mathscr{A}_{DK^*} \equiv \frac{\mathscr{B}(\bar{B}^0\to[K^+\pi^-]_D K^-\pi^+)-\mathscr{B}(B^0\to[K^-\pi^+]_D K^+\pi^-)}{\mathscr{B}(\bar{B}^0\to[K^+\pi^-]_D K^-\pi^+)+\mathscr{B}(B^0\to[K^-\pi^+]_D K^+\pi^-)} = 2kr_S r_D \sin(\delta_S+\delta_D)\sin\phi_3/\mathscr{R}_{DK^*}, \quad (5.7)$$

where the parameters r_S, δ_S and k are defined as

$$r_S^2 \equiv \frac{\Gamma(B^0\to D^0K^+\pi^-)}{\Gamma(B^0\to \bar{D}^0K^+\pi^-)} = \frac{\int dp A^2_{b\to u}(p)}{\int dp A^2_{b\to c}(p)}, \quad (5.8)$$

$$k e^{i\delta_S} \equiv \frac{\int dp A_{b\to c}(p) A_{b\to u}(p) e^{i\delta(p)}}{\sqrt{\int dp A^2_{b\to c}(p) \int dp A^2_{b\to u}(p)}}. \quad (5.9)$$

Here $A_{b\to c}(p)$ and $A_{b\to u}(p)$ are the magnitudes of the amplitudes for the $b\to c$ and $b\to u$ transitions, respectively, and $\delta(p)$ is the relative strong phase. The variable p indicates the position in the $DK^+\pi^-$ Dalitz plot. In this analysis, we calculate the integrals over a phase space of the state $DK^*(892)^0$. The value of r_S is expected to be around 0.4, which is obtained from $|V_{ub}V^*_{cs}|/|V_{cb}V^*_{us}|$, and depends on strong interaction effects. According to a simulation study using a Dalitz model based on recent measurements [20], the value of k is around 0.95 in the phase space of interest here.

Belle has performed a measurement on $\bar{B}^0\to D\bar{K}^{*0}$ based on the full dataset that contains 772×10^6 $B\bar{B}$ pairs [21]. In this result, most stringent limit on $\mathscr{R}_{DK^*}$ is obtained. Figure 9 shows the fit result. We obtain $\mathscr{R}_{DK^*} = (4.5^{+5.6+2.8}_{-5.0-1.8})\times10^{-2}$ and set a credible upper limit at 95% $\mathscr{R}_{DK^*} < 0.16$.

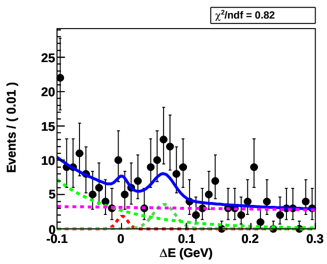

Figure 9: (color online) Fit result of ΔE distribution for $\bar{B}^0\to[K^+\pi^-]_D\bar{K}^{*0}$, where the charge conjugate mode is included. Signal component (red) is located at around $\Delta E = 0$ GeV, $\bar{B}^0\to D\rho^0$ component (magenta) is located at around $\Delta E = 0.05$ GeV, and $B\bar{B}$ (green) and $q\bar{q}$ (blue) background components are located in the entire region.

6. Summary

I review some measurements related to the angles of the unitarity triangle. In ϕ_1 measurements, the time-dependent CP violation measurement with $B^0\to(c\bar{c})K^0$ modes are updated. In ϕ_2

measurements, a measurement of the product branching fraction and time-dependent parameters in $B^0 \to a_1(1260)^{\pm}\pi^{\mp}$ decays is performed, where we obtain the first evidence of the mixing-induced *CP* violation. In ϕ_3 measurements, the model-independent Dalitz plot analysis in $B^- \to [K_S\pi\pi]_D K^-$ is preformed, and a measurement in $B^0 \to [K\pi]_D K^{*0}$ decays analysis is newly achieved.

References

[1] N. Cabibbo, Phys. Rev. Lett. **10**, 531 (1963); M. Kobayashi and T. Maskawa, Prog. Theor. Phys. **49**, 652 (1973).

[2] L. Wolfenstein, Phys. Rev. Lett. **51**, 1945 (1983).

[3] A. B. Carter and A. I. Sanda, Phys. Rev. D **23**, 1567 (1981); I. I. Bigi and A. I. Sanda, Nucl. Phys. B **193**, 85 (1981).

[4] I. Adachi *et al.* (Belle collaboration), Phys. Rev. Lett. **108**, 171802 (2012).

[5] H. Kakuno *et al.*, Nucl. Instrum. Methods Phys. Res., Sect. A **533**, 516 (2004).

[6] H. Tajima *et al.*, Nucl. Instrum. Methods Phys. Res., Sect. A **533**, 370 (2004).

[7] M. Gronau and D. London, Phys. Rev. Lett. **65** 3381 (1990).

[8] M. Gronau and J. Zupan, Phys. Rev. D. **73** 057502 (2006).

[9] J. Charles *et al.* (CKMfitter Group), Eur. Phys. J. C **41**, 1 (2005), and online update at http://ckmfitter.in2p3.fr.

[10] J. Dalseno *et al.* (Belle Collaboration), arXiv:1205.5957 (2012).

[11] A. Giri, Yu. Grossman, A. Soffer and J. Zupan, Phys. Rev. D **68**, 054018 (2003); A. Bondar, Proceedings of BINP Special Analysis Meeting on Dalitz Analysis, 2002 (unpublished).

[12] A. Poluektov *et al.* (Belle Collaboration), Phys. Rev. D **81**, 112002 (2010).

[13] H. Aihara *et al.* (Belle Collaboration), Phys. Rev D **85**, 112014 (2012).

[14] R. A. Briere *et al.* (CLEO Collaboration), Phys. Rev. D **80**, 032002 (2009); J. Libby *et al.* (CLEO Collaboration), Phys. Rev. D **82**, 112006 (2010).

[15] M. Gronau and D. London, Phys. Lett. B **253**, 483 (1991); M. Gronau and D. Wyler, Phys. Lett. B **265**, 172 (1991).

[16] Belle Collaboration, Lepton Photon 2011 preliminary.

[17] D. Atwood, I. Dunietz and A. Soni, Phys. Rev. Lett. **78**, 3257 (1997); Phys. Rev. D **63**, 036005 (2001).

[18] D. Asner *et al.* (Heavy Flavor Averaging Group), arXiv:1010.1589, and online update at http://www.slac.stanford.edu/xorg/hfag.

[19] Y. Horii *et al.* (Belle Collaboration), Phys. Rev. Lett. **106**, 231803 (2011).

[20] B. Aubert *et al.* (BaBar Collaboration), Phys. Rev. D **79**, 072003 (2009).

[21] K. Negishi *et al.* (Belle Collaboration), Phys. Rev. D **86**, 011101 (2012).

PoS(HQL 2012)040